Robust Wireless Power Transfer: A Self-Adaptive Approach

Fu Liu,* Bhakti Chowkwale, Prasad Jayathurathnage, Sergei Tretyakov

Department of Electronics and Nanoengineering, Aalto University,
P. O. Box 15500, FI-00076 Aalto, Finland
*E-mail: fu.liu@aalto.fi

Abstract

While wired power transfer devices ensure robust power delivery even if the receiver position or load impedance change, achieving the robustness of wireless power transfer is challenging. Conventional solutions are based on additional feedback circuits for dynamical tuning of the link parameters. Here, we propose a robust wireless power transfer paradigm that works for a wide range of load and receiver positions. It realizes a virtual, nearly ideal oscillating voltage source at the load site, comparable to the wired connection. The operating frequency is automatically adopted to the optimal working condition under the changes of load and receiver positions. We experimentally verify the robustness of the system. The working frequency and the transferred power agrees well with our analytical models. We discuss the practical limitations and suggest directions for future developments.

Introduction

The concept of wireless power transfer (WPT) was patented by N. Tesla about 100 years ago [1]. Ever since, researchers and engineers have been investigating methods for improving WPT technologies in terms of efficiency, power, transmission distance, human safety, and adaptive tuning aspects [2, 3, 4, 5, 6]. Recently, WPT technologies have been widely adopted to many applications including consumer electronics [7], biomedical implants [8, 9], industrial applications, and electric vehicles [10, 11]. A typical WPT system consists of a microwave generator, a transmitter, and a receiver that is separated from transmitter and connected to the load [2]. Energy is transferred from the transmitter to the receiver via a wireless link either using inductive coupling (magnetic field) [2, 3, 4] or capacitive coupling (electric field) [11, 12, 13, 14]. The optimal power transfer occurs when the frequency and load are chosen to operate at the conjugate matched condition. However, in practical applications, variations in working conditions such as the receiver position (coupling strength) and load are inevitable, and deviate the system from optimal operation [4]. As such, a WPT system optimized for a nominal working condition may not function optimally, and the system components need to be continuously tuned to achieve the conjugate matched condition [4, 15, 16, 17]. Therefore, the robustness, which is the ability to operate in the optimal regime without any additional tuning under system variations, is a very crucial performance criterion for WPT systems.

Recent developments demonstrate that parity-time symmetric WPT systems can be robust against coupling variations within the strong coupling region [18, 19], but realization of negative resistance using impedance inverters or other means is inherently a low-efficiency process [18, 20]. In paper [19], a generic on-site WPT scheme, which ensures operation robustness by generating oscillations directly at the load itself and does not suffer from the low efficiency of negative-resistance circuits, has been theoretically proposed. In this work, based on the self-oscillating circuit scenario, we realize a robust on-site WPT system that automatically adjusts itself to the optimal regime although the load resistance and the receiver position vary in a wide range. Under certain conditions, the proposed WPT system behaves nearly equivalent to the direct wired connection to the load.

Conventional versus on-site WPT systems

A comparison of the conventional WPT system and the on-site WPT is illustrated in Fig. 1, using capacitive WPT as an example. In conventional devices, the generator, transmitter and receiver are functionally distinct. The utility power is first converted to microwave power by using a generator since DC or 50-60 Hz power cannot be effectively transferred via free space. Next, the output microwave power is delivered from the transmitter to receiver through capacitive coupling. The operating conditions of the generator are determined by its circuitry, therefore, the transferred power alters with the variation of the load and the receiver positions. Conversely, in the proposed on-site generation WPT paradigm, the load and the wireless power link are parts of the positive feedback loop, forming a unified oscillator circuit. The microwave power is therefore directly generated at the load position, as shown in Fig. 1(b). The feedback loop passing through the coupling capacitance and the load determines the oscillation frequency by itself. In this way, no additional tuning circuitry is needed to maintain the optimal condition.

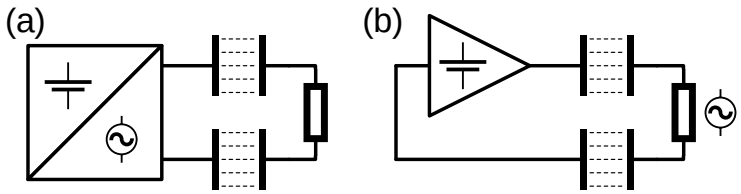

Figure 1: Comparison between the conventional and the proposed WPT systems. (a) In conventional ones, the microwave oscillation is formed in the generator and then transmitted to the load through capacitive wireless link. (b) In the proposed WPT system, the wireless link and the load are part of the feedback loop and the oscillating power is directly generated at the load.

A particular example of proposed self-adaptive WPT systems using an operational amplifier (op-amp) [21, 22] is suggested and depicted in Fig. 2(a), along with the definitions of the variables. In this system, two identical parallel-plate capacitors C_{p} provide the wireless link for transferring energy to the load R_{L} as well as a positive feedback loop to maintain self-oscillations. Example oscillations from simulation (LTspice IV, same for the following simulations) are shown as solid lines in Fig. 2(b). If the receiver is removed, the feedback loop is disconnected, therefore there is no oscillation. This brings a significant advantage of automatic receiver detection which greatly reduces stand-by losses.

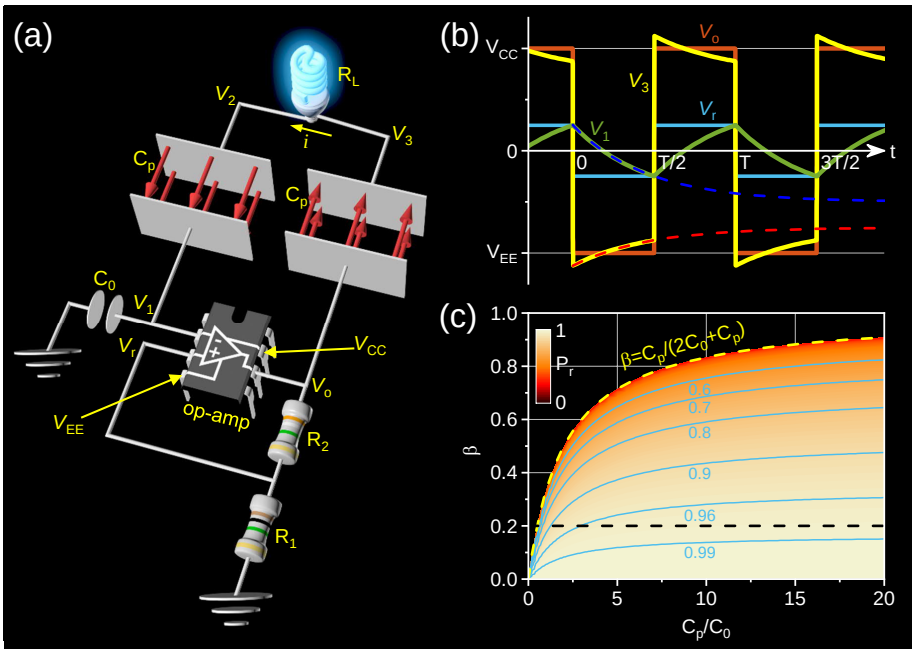

Figure 2: The proposed WPT system based on self-oscillating circuit and its theoretical operation. (a) Schematic of the WPT system with variable definitions. The feedback loops at inverting (-) and non-inverting (+) terminals make the output oscillate thus drive the energy wirelessly to the load. (b) Voltage oscillations from simulation (solid lines) and analytical solutions of V_1 and V_3 in Eqs. 1 and 2 (dashed lines). (c) Analytical power ratio P_r as a function of C_p/C_0 and β. The yellow dashed line indicates the boundary of the oscillation. The system operates closer to the wired case when the configuration is further away from the boundary. The black dashed line is for $\beta = 0.2$.

Theoretical model of the proposed WPT system

The analytical solution for the proposed WPT system is derived based on the assumption that the op-amp is ideal. From Kirchhoff's law, we obtain the time-dependent solutions for V_1 and V_3

$$V_1(t) = \frac{V_\mathrm{CC}}{2C_0 + C_\mathrm{p}} \left[(C_\mathrm{p} + 2C_0\beta + C_\mathrm{p}\beta) e^{-t/\tau} - C_\mathrm{p} \right], \quad (1)$$

$$V_3(t) = -\frac{V_\mathrm{CC}}{2C_0 + C_\mathrm{p}} \left[(C_\mathrm{p} + 2C_0\beta + C_\mathrm{p}\beta) e^{-t/\tau} C_0/C_\mathrm{p} + C_\mathrm{p} + C_0 \right], \quad (2)$$

for the first half period ($0 \le t < T/2$), where $\beta = R_1/(R_1 + R_2)$ is the voltage division, $\tau = C_0 C_\mathrm{p} R_\mathrm{L}/(2C_0 + C_\mathrm{p})$ is the characteristic time, and we have adopted $V_\mathrm{EE} = -V_\mathrm{CC}$ for symmetric operation. For the second half period ($T/2 \le t < T$), the solution can be found

by simply changing $V_{\rm CC}$ to $V_{\rm EE}$ and t to $t - T/2$. Both V_1 and V_3 change exponentially, following the charge and discharge processes, and they are plotted in Fig. 2(b) as dashed curves (blue for V_1 and red for V_3), complementing the simulation results. The oscillation period T is obtained as

$$T = 2\frac{C_0 C_{\rm p} R_{\rm L}}{2C_0 + C_{\rm p}} \ln\left[\frac{C_{\rm p} + (2C_0 + C_{\rm p})\beta}{C_{\rm p} - (2C_0 + C_{\rm p})\beta}\right] \tag{3}$$

through the switch condition $V_1(T/2) = \beta V_{\rm EE}$. However, the condition $V_1(t \to \infty) < \beta V_{\rm EE}$ must be satisfied to support the oscillations. This gives the oscillation condition

$$\beta < \frac{C_{\rm p}}{2C_0 + C_{\rm p}}. \tag{4}$$

As long as the system parameters satisfy this condition, power will be wirelessly delivered to the load, meaning that the proposed WPT system is robust.

At the same time, with $V_2 = (C_{\rm p} + C_0)V_1/C_{\rm p}$, the average power delivered to the load can be calculated by $1/T \int_0^T (V_3 - V_2)^2/R_{\rm L} {\rm d}t$, which results in

$$P_{\rm avg} = \frac{V_{\rm CC}^2}{R_{\rm L}} \frac{2(2C_0 + C_{\rm p})\beta}{C_{\rm p}} \Big/ \ln\left[\frac{C_{\rm p} + (2C_0 + C_{\rm p})\beta}{C_{\rm p} - (2C_0 + C_{\rm p})\beta}\right]. \tag{5}$$

We notice that the first term $P_0 = V_{\rm CC}^2/R_{\rm L}$ is the power consumed by the load if we were to connect the load directly to the source voltage $V_{\rm CC}$. Thus, the value of P_0 provides a very good performance reference and we define a power ratio

$$P_{\rm r} = P_{\rm avg}/P_0 \tag{6}$$

to measure how well the WPT system performs compared to the direct wired connection. We highlight that $P_{\rm r}$ is not a function of the load resistance $R_{\rm L}$, meaning that the power ratio is robust against the changes of the load. Figure 2C shows the analytical contour plot of $P_{\rm r}$ as a function of $C_{\rm p}/C_0$ and β. As we can see, it is bounded by the oscillation condition in Eq. 4. When the system parameters $(C_{\rm p}/C_0, \beta)$ move way from the boundary, $P_{\rm r}$ increases and can achieve 0.99 for small β. This means that the performance of the proposed WPT system is comparable to the wired connection. More importantly, with constant β, $P_{\rm r}$ is insensitive for large $C_{\rm p}/C_0$, indicating that we can obtain efficient and robust WPT with high $P_{\rm r}$ for a broad range of plate capacitances, that is, for varying transfer distance. For example, if we choose $\beta = 0.2$, we can achieve $P_{\rm r} > 0.9$ when $C_{\rm p}/C_0 > 1.23$.

Actually, the simplifying assumption of the identical plate capacitors is not necessary, and the system is still robust when they have different capacitances. The power ratio remains almost unchanged when the two plate capacitances deviate from each other. This is of great advantage in WPT applications as misalignment of the receiving plates will not significantly affect the WPT operation.

We emphasize that, in principle, the proposed WPT system can work for any value of load resistance and plate capacitance as long as the oscillation condition Eq. 4 is satisfied. In actual implementations, it means that energy can be transferred to any load with any distance and misalignment between the metal plates within the boundaries set by Eq. 4.

Experimental demonstration of the power transfer robustness

We experimentally demonstrate the robustness of the proposed WPT system with a specific op-amp (TL051CP). The experimental setup is shown in Fig. 3(a) with the system parameters $R_1 = 1$ MΩ, $R_2 = 3.9$ MΩ, $C_0 = 4.7$ nF, and $V_{\mathrm{CC/EE}} = \pm 12V$. The wireless link is realized with two pairs of aluminium plates with width w = 30 cm and length $L = 50$ cm. Each pair of plates is separated by distance $d = 0.1$ mm (paper with relative permittivity $\epsilon_r = 1.4$) to provide the plate capacitance in the nF range, appropriate for the parameters of the selected op-amp. The three characteristic voltages V_{o}, V_2, and V_3 are measured with a high speed oscilloscope [23]; then the data is processed to determine the oscillation frequency $f = 1/T$ and the power ratio. The robustness of the WPT system is demonstrated by varying both the load resistance R_{L} and the receiver position (the plate capacitance C_{p}).

We first demonstrate the robustness with respect to changes of the load resistance R_{L}. The capacitance of the aluminium plates is measured to be 18.1 nF. In theory, this configuration should work for arbitrary R_{L} values. However, the maximum oscillating frequency supported by the selected op-amp defines the lower bound of R_{L} to be approximately 400 Ω. Therefore, we vary R_{L} from 470 Ω to 4.7 MΩ and the measured frequencies are shown in Fig. 3(b). It is clear that the experimental and simulation results [24] acknowledge each other very well and the frequency is inversely proportional to R_{L}, following the analytical black line defined by Eq. 3. In calculating the power ratio, we note that the magnitude of the V_{o} swing is less than the feeding voltages (inset of Fig. 3(c)).

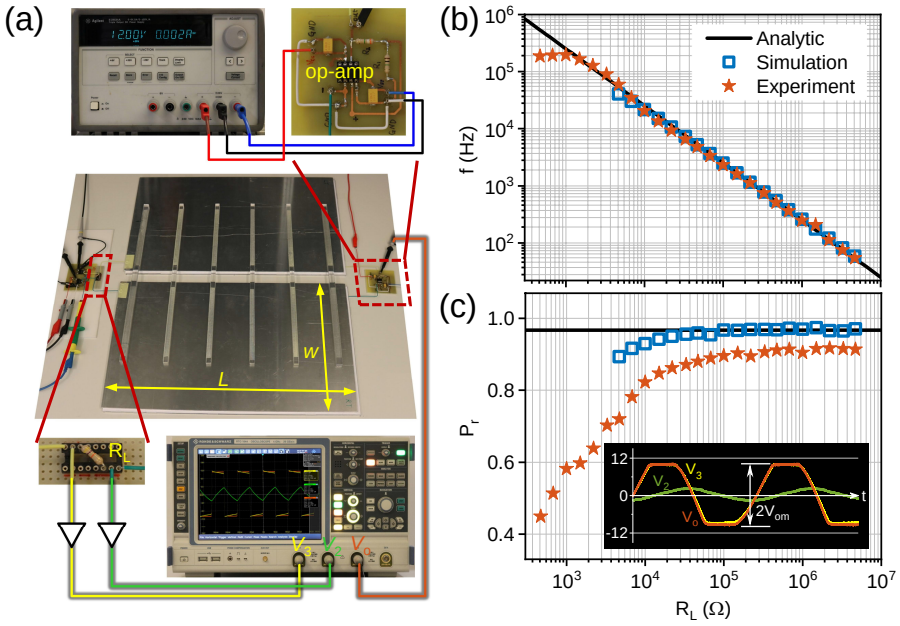

Figure 3: Experimental demonstration of the robustness against load variation. (a) Experimental setup. The capacitive wireless links are made of aluminum plates. (b) Working frequency is inversely proportional to load resistance. (c) Power ratio versus load resistance. The measured value drops when load resistance decreases. The insert shows the experimental voltage oscillations when $R_{\mathrm{L}} = 1.5$ kΩ.

Therefore, to give comparable results to the analytical solutions, we calculate the power ratio by $P'_{\mathrm{r}} = P_{\mathrm{avg}}/P'_0$ where $P'_0 = V_{\mathrm{m}}^2/R_{\mathrm{L}}$ and $2V_{\mathrm{m}}$ is the measured peak to peak voltage of the output. The corresponding power ratios from experiments and simulations are shown in Fig. 3(c). They agree well with the analytical solution with an exception for low R_{L} values. The discrepancy comes from the finite slew rate of the selected op-amp which prohibits instant switching of the output (inset of Fig. 3(c)).

We then demonstrate the robustness with respect to the changes of the receiver position. We modify the overlap area by sliding the top plates (inset of Fig. 4(a)). The plate capacitance C_{p} is therefore a linear function of the overlap distance l, and the measured capacitances are shown in Fig. 4(a) when we range l from 10 cm to 50 cm. We perform the experiments with five load values, i.e., 1 kΩ, 3.3 kΩ, 10 kΩ, 33 kΩ, and 100 kΩ. The measured frequencies and power ratios are shown in Figs. 4B and C as symbols, while the lines are obtained from the analytical solutions. As we can observe, the WPT system operates robustly while changing the receiver position. For a fixed load, the working fre-

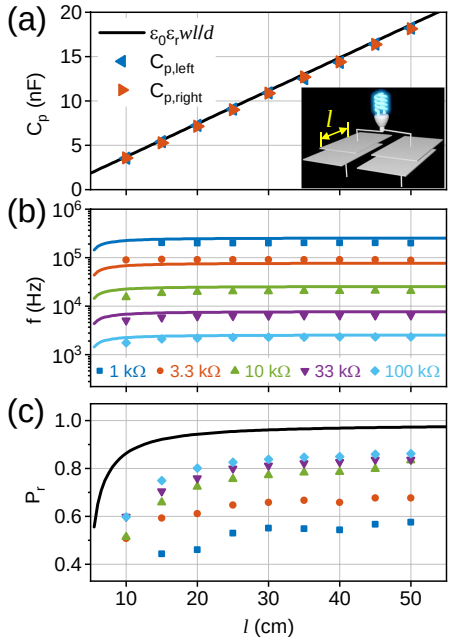

Figure 4: Experimental demonstration of the robustness against receiver position (overlap distance). (a) The plate capacitance is linearly proportional to the overlap distance l of the aluminum plates. The inset shows how the plates are moved. (b, c) Measured (symbols) and analytic (lines) working frequency and power ratio subjected to the changes of overlap distance. Five load values are measured.

quency is almost constant, while the power ratio increases, subject to the change of the overlap distance. These results are consistent with the aforementioned ones in Fig. 3.

Moreover, the robustness of the WPT system is also experimentally verified by moving and rotating the receiving part while the WPT system is on. For visualization, two LEDs, accompanying the load, are glowing while the position of the receiving part changes.

Discussions and conclusions

The proposed on-site wireless power generation paradigm based on the self-adaptive concept realizes a virtual, nearly ideal voltage source at the position of the power-receiving load. Under certain conditions, this voltage source is comparable to the wired connection case, enabling efficient and robust wireless power delivery. As the load and the capacitive wireless link are parts of the feedback loop of a self-oscillating circuit, the proposed WPT system automatically adjusts itself to the optimal working condition and provides

robust operation against changes of the receiving end, including the load resistance and the receiver position. No additional tuning circuit is required to maintain the system in resonance which is needed in conventional WPT systems.

In the proposed WPT system, there is no inevitable loss in the output resistance of the generator as this output resistance is now the useful load itself. In our example realization the dissipation losses in R_1 and R_2 are negligible, and parasitic losses occur only in the op-amp acting as a switch, which are also present in all conventional systems. Moreover, the conventional definition of WPT efficiency, which is the ratio of the power delivered to the load and the output power of the oscillator [3, 18], makes no sense here as it is always 100%. The only proper measure of the efficiency applicable to all WPT systems including the proposed one is the overall efficiency, which can be defined by the ratio between the power consumption in the load and the total power taken from the utility source, i.e., $\eta = P_{\text{avg}}/P_{\text{in}}$. In our demonstration, the maximum overall efficiency of 36.7% is observed. The moderate overall efficiency is due to the comparably large parasitic losses in the selected op-amp.

Comparing with the load-independent power ratio (Eqs. 5 and 6) of the proposed WPT system, the conventional WPT system is less robust as its power ratio is strongly load-dependent. This load dependence diminishes the wireless power delivery at small load values. We believe that the efficiency, load range, and transfer distance can substantially enhanced with better characteristic op-amps or using other active components. The WPT system proposed here has generally no fundamental limitations.

Acknowledgments

We thank Matti Vaaja for technical help with the experimental equipment and Viktar Asadchy for making the schematics. This work was supported by the European Unions Horizon 2020 research and innovation programme-Future Emerging Topics (FETOPEN) under grant agreement No 736876.

References

[1] Tesla, N. Apparatus for transmitting electrical energy (1914).

[2] Hui, S. Y. R., Zhong, W. & Lee, C. K. A critical review of recent progress in mid-range wireless power transfer. *IEEE Transactions on Power Electronics* **29**, 4500–4511 (2014).

[3] Kurs, A. *et al.* Wireless power transfer via strongly coupled magnetic resonances. *Science* **317**, 83–86 (2007).

[4] Sample, A. P., Meyer, D. A. & Smith, J. R. Analysis, experimental results, and range adaptation of magnetically coupled resonators for wireless power transfer. *IEEE Trans. Ind. Electron.* **58**, 544–554 (2011).

[5] Christ, A. *et al.* Evaluation of wireless resonant power transfer systems with human electromagnetic exposure limits. *IEEE Transactions on Electromagnetic Compatibility* **55**, 265–274 (2013).

[6] Song, M., Belov, P. & Kapitanova, P. Wireless power transfer inspired by the modern trends in electromagnetics. *Applied Physics Reviews* **4**, 021102 (2017).

[7] Chao, W.-C. Battery charging device for mobile phone (2000).

[8] Kakegawa, M. Apparatus for transmitting energy to a device implanted in a living body (1984).

[9] Ho, J. S. *et al.* Wireless power transfer to deep-tissue microimplants. *Proceedings of the National Academy of Sciences* **111**, 7974–7979 (2014).

[10] Vilathgamuwa, D. M. & Sampath, J. P. K. Wireless power transfer (WPT) for electric vehicles (EVs)—present and future trends. In *Plug In Electric Vehicles in Smart Grids*, 33–60 (Springer Singapore, 2014).

[11] Dai, J. & Ludois, D. C. Wireless electric vehicle charging via capacitive power transfer through a conformal bumper. In *2015 IEEE Applied Power Electronics Conference and Exposition (APEC)* (IEEE, 2015).

[12] Kline, M., Izyumin, I., Boser, B. & Sanders, S. Capacitive power transfer for contactless charging. In *2011 Twenty-Sixth Annual IEEE Applied Power Electronics Conference and Exposition (APEC)* (IEEE, 2011).

[13] Dai, J. & Ludois, D. C. Single active switch power electronics for kilowatt scale capacitive power transfer. *IEEE Journal of Emerging and Selected Topics in Power Electronics* **3**, 315–323 (2015).

[14] Lu, F., Zhang, H., Hofmann, H. & Mi, C. C. A double-sided LC-compensation circuit for loosely coupled capacitive power transfer. *IEEE Transactions on Power Electronics* **33**, 1633–1643 (2018).

[15] Beh, T. C., Kato, M., Imura, T., Oh, S. & Hori, Y. Automated impedance matching system for robust wireless power transfer via magnetic resonance coupling. *IEEE Transactions on Industrial Electronics* **60**, 3689–3698 (2013).

[16] Duong, T. & Lee, J.-W. A dynamically adaptable impedance-matching system for midrange wireless power transfer with misalignment. *Energies* **8**, 7593–7617 (2015).

[17] Liu, S., Liu, M., Han, S., Zhu, X. & Ma, C. Tunable class E^2 DC-DC converter with high efficiency and stable output power for 6.78-MHz wireless power transfer. *IEEE Transactions on Power Electronics* **33**, 6877–6886 (2018).

[18] Assawaworrarit, S., Yu, X. & Fan, S. Robust wireless power transfer using a nonlinear parity–time-symmetric circuit. *Nature* **546**, 387–390 (2017).

[19] Ra'di, Y. *et al.* On-site wireless power generation. *IEEE Transactions on Antennas and Propagation* 1–1 (2018). Early Access: https://doi.org/10.1109/TAP.2018.2835560.

[20] Pozar, D. M. *Microwave Engineering* (Wiley, 2011).

[21] Graeme, J. G. *Applications of Operational Amplifiers: Third Generation Techniques (The BB electronics series)* (McGraw-Hill, 1973).

[22] Sedra, A. S. & Smith, K. C. *Microelectronic Circuits 5TH Edition* (McGraw-Hill, 2004).

[23] The voltages V_2 and V_3 are measured through a buffer made from the same op-amp.

[24] The LTSpice model of the op-amp is downloaded from http://www.ti.com/product/TL051/toolssoftware. When the load resistance R_{L} is smaller than 4.7 kΩ, the simulation fails.